JACS
JOURNAL OF THE AMERICAN CHEMICAL SOCIETY

ARTICLE

pubs.acs.org/JACS

Potential Energy Surface for (Retro-)Cyclopropanation: Metathesis with a Cationic Gold Complex

Alexey Fedorov, Laurent Batiste, Andreas Bach, David M. Birney,[†] and Peter Chen*

Laboratorium für Organische Chemie, ETH Zürich, Wolfgang-Pauli-Strasse 10, CH−8093 Zürich, Switzerland

Supporting Information

ABSTRACT: The gas-phase cyclopropanation and apparent metathesis reactivity of ligand-supported gold arylidenes with electron-rich olefins is explained by quantum-chemical calculations. A deep potential minimum corresponding to a metal-bound cyclopropane adduct is in agreement with the measured absolute energies of the cyclopropanation and metathesis channels and is also consistent with previously reported electronic effects of arylidenes and supporting phosphorus ylid ligands on the product ratios. In the gas phase, the rate-determining step for the cyclopropanation is dissociation of the Lewis-acidic metal fragment, whereas the metathesis pathway features several rate-limiting transition states that are close in energy to the final product dissociation and hence contribute to the overall reaction rate. Importantly, the presented potential energy surface also accounts for the recently reported gold-catalyzed solution-phase retro-cyclopropanation reactivity.

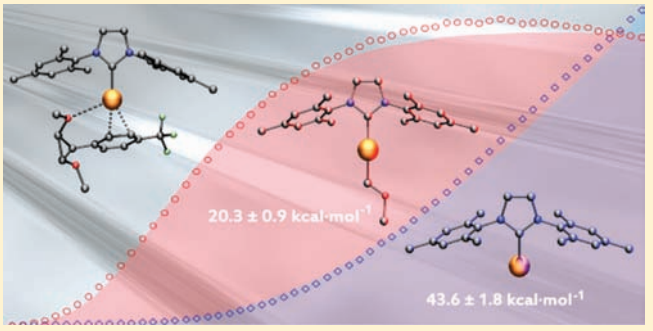

INTRODUCTION

Since the acceptance of the Chauvin mechanism[1] for olefin metathesis in preference to those originally suggested by Calderon,[2] Pettit,[3] and Grubbs,[4] no new mechanistic concepts for this process have appeared in the literature. That being said, early investigations on tungsten-mediated metathesis reactions suggested that cyclopropanes might serve as a reservoir species for active metathesis catalysts.[5] In this report, we detail our mechanistic studies on what appeared to be a metathesis reaction of gold carbene complexes with electron-rich olefins, but which constitutes another example of a system that does not follow a Chauvin-type carbene exchange pathway, instead featuring metal-bound cyclopropane species as progenitors to new carbene complexes.

Our recent experimental and computational work on gold carbenes implicated a stepwise process for gold-mediated cyclopropanation and apparent metathesis pathways[6−8] and allowed us to predict that transcyclopropanation and cyclopropane metathesis reactions may be brought about via catalysis with cationic d[10] coinage metal complexes.[7b] The potential energy surface (PES) presented below confirms our previous claims and indicates useful access points to yield such reactivity in solution.

EXPERIMENTAL AND COMPUTATIONAL DETAILS

Quantum-chemical calculations were performed with the Gaussian09 suite[9] employing the PW91 density functional in combination with the cc-pVDZ-PP small-core relativistic correlation-consistent basis set[10] for gold and cc-pVDZ for the remaining elements. For all the stationary points and transition states except $\mathbf{TS_{11-12}}$, geometry optimizations were performed with tight SCF and convergence criteria and an ultrafine integration grid. The nature of each stationary point was confirmed by a frequency analysis, which also afforded the zero-point energy (ZPE) correction.

Mass spectrometric measurements were performed on a Finnigan MAT TSQ-700 instrument, in which the first transfer octopole has been replaced by a custom-made 24-pole ion guide.[11] Energy-resolved reactive cross-section[12] measurements were executed as described earlier.[11] Species of interest were prepared and thermalized in the first 24-pole ion guide to a temperature of 343 K using *cis*-dimethoxyethylene (ca. 10 mTorr), and mass selected by the first quadrupole. They were then reacted with xenon in the octopole collision cell while monitoring the products as a function of collision energy.

The "daughter" mode was used for mass selection, and a retarding potential measurement of the kinetic energy distribution of the ions was performed before each experiment, yielding approximately Gaussian distributions. The resolution for parent-ion selection was always kept high enough to ensure that fragmentation in the daughter mode occurs only for the ions of interest. Reactive cross sections were determined at 40−100 μTorr pressure of xenon collision gas and linearly extrapolated to zero pressure to impose strict single-collision conditions. Three independent data sets were obtained and the activation energy was extracted from the reactive cross sections using the program L-CID.[13] The density-of-states model used by L-CID requires an input specification of the number of rotors in the molecule; we assumed a total of 9 rotors. The reported error bounds include the standard deviation computed from 15 best fits per data set and a 0.15 eV (lab frame) uncertainty on the absolute energy scale.

For the kinetic isotope effect measurements, 3 independent data sets were collected containing 10 spectra per given experimental conditions while every spectrum was an average of 120 scans. Peak areas were

Received: May 6, 2011
Published: June 22, 2011

dx.doi.org/10.1021/ja2041699 | *J. Am. Chem. Soc.* 2011, 133, 12162–12171

integrated and normalized against the overall ion current. We assumed that ion intensities are directly proportional to reaction rates.

RESULTS

Recently, we reported an experimental reactivity study of an IMes-supported (IMes = 1,3-bis(2,4,6-trimethylphenyl)imidazol-2-ylidene) cationic gold benzylidene complex, which was prepared inside a mass-spectrometer from the phosphorus ylid adduct (Scheme 1).[6−8,14] The fact that metathesis reactivity is observed only with electron-rich olefins and not with, for example, 3-hexene[6] is not expected from the Chauvin mechanism and thus indicates that another mechanism might be operative. Furthermore, collision-induced dissociation (CID) experiments and DFT calculations on a methoxy-substituted model cyclopropane system demonstrated that a new gold Fischer carbene complex can be obtained from a metal-bound cyclopropane adduct.[8] The simultaneously occurring metathesis and cyclopropanation channels rendered the system information-rich and structure-sensitive,[15] as was further studied by monitoring intensity changes of the exit channels as a function of electronic perturbations on the benzylidene fragment[7a] or the supporting P-ylid ligand.[7b]

Threshold CID Experiments. Under suitable electrospray ionization (ESI) conditions the corresponding ylid precursor[14] (Scheme 1, Ar = *p*-$CF_3C_6H_4$) affords trifluoromethyl-substituted benzylidene complex **1**, which forms an adduct with *cis*-dimethoxyethylene **2** in the gas phase. Regeneration of the starting arylidene from this adduct (*m*/*z* 747, Figure 1) via collision-induced olefin loss is substantially suppressed, which renders the system suitable for two-channel energy-resolved threshold CID (T-CID) measurement of the cyclopropanation and metathesis processes (Figure 2)[15−17] to afford reference thermochemical information for the validation of the computational method. Thus, the experimental results presented below are obtained under the assumption that the presence of the former minor channel does not significantly influence the cross sections of the reactions of interest.

Scheme 1. Previously Reported Studies of Gold-Mediated Cyclopropanation and Metathesis

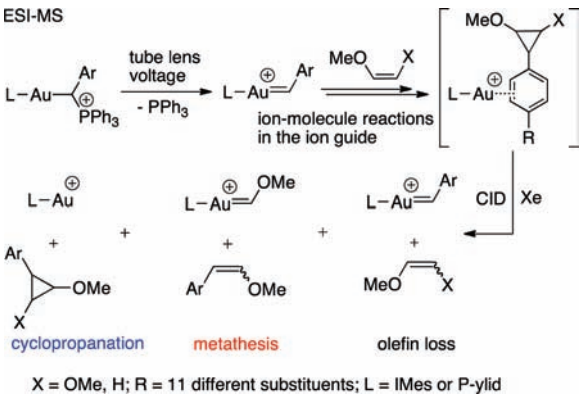

Activation energies for cyclopropanation and metathesis were extracted by fitting the zero-pressure extrapolated reactive cross section curves with the L-CID program (Figure 2).[13] To correctly account for the kinetic shift that is inherent to T-CID measurements, the fitting process of L-CID requires an input assumption of the transition-state model for each channel under investigation. A "tight" fitting model should be chosen if an intramolecular rearrangement is rate-determining, whereas a "loose" model is appropriate when the rate-limiting process is product dissociation, that is, with merely a centrifugal barrier for the reverse process.[13,18] Since electronic perturbation at the arylidene moiety resulted in different slopes in Hammett plots for the cyclopropanation and metathesis channels and since the product ratio depended on the collision energy, one can rule out a common rate-determining transition state for these processes.[7a]

Furthermore, the intensity of the LAu^+ (L = IMes or P-ylid) signal rapidly increases with collision energy in excess of the reaction threshold.[6,7] This behavior is characteristic of a simple ligand dissociation, which was also confirmed by the DFT calculations (*vide infra*). Therefore, the fitting of the cross-section data for the cyclopropanation manifold was conducted with a loose transition-state model.[19] Likewise, the excellent agreement of the computational results for the metathesis channel with the fitted values using a tight transition-state model renders the latter assumption legitimate (*vide infra*).[20] Thus, experimental reaction barriers of 43.6 ± 1.8 kcal mol^{-1} for the cyclopropanation and 20.3 ± 0.9 kcal mol^{-1} for the apparent metathesis process were obtained from L-CID using a loose and a tight TS model, respectively.

Kinetic Isotope Effect Study. Our group has previously reported k^H/k^D values in the range of 0.68 to 0.8 and 0.92 for acyclic metathesis with Ru benzylidenes and olefins such as ethyl vinyl ether or 1-butene.[21] This inverse secondary kinetic isotope effect is characteristic for the $sp^2 \rightarrow sp^3$ rehybridization occurring upon formation of a metallacyclobutane from the ruthenium carbene and the olefin. In order to examine whether similar effects occur for gold carbenes, we compared relative product

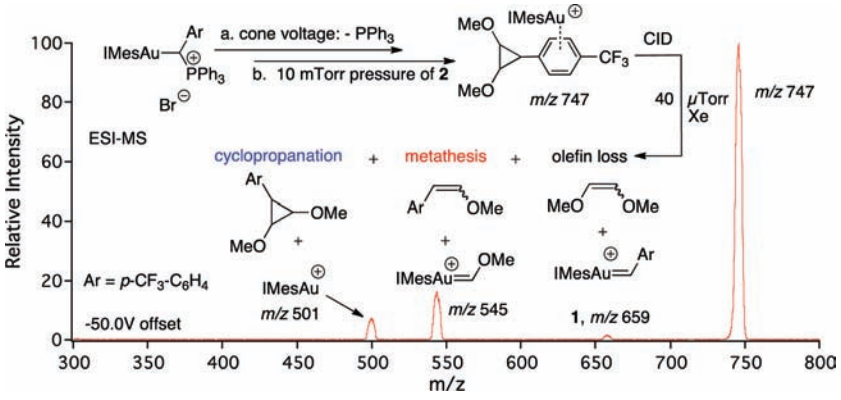

Figure 1. Daughter-ion spectrum obtained by mass selection of the adduct at *m*/*z* 747, formed by gas-phase reaction of **1** with *cis*-dimethoxyethylene (**2**), and subsequent collision with 40 μTorr xenon at −50.0 V collision offset (lab frame), featuring the cyclopropanation and metathesis exit channels.

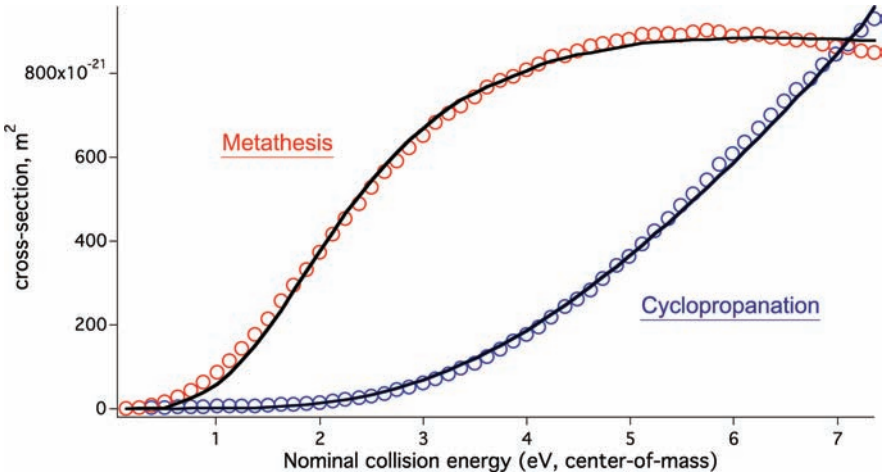

Figure 2. Linearly zero-pressure extrapolated, energy-resolved reactive cross sections as measured for the appearance of $IMesAu^+$ (m/z 501, blue circles) and $IMesAuCHOMe^+$ (m/z 545, red circles), and L-CID fits (black lines), assuming a loose transition-state model for the cyclopropanation and a tight one for the metathesis, respectively.

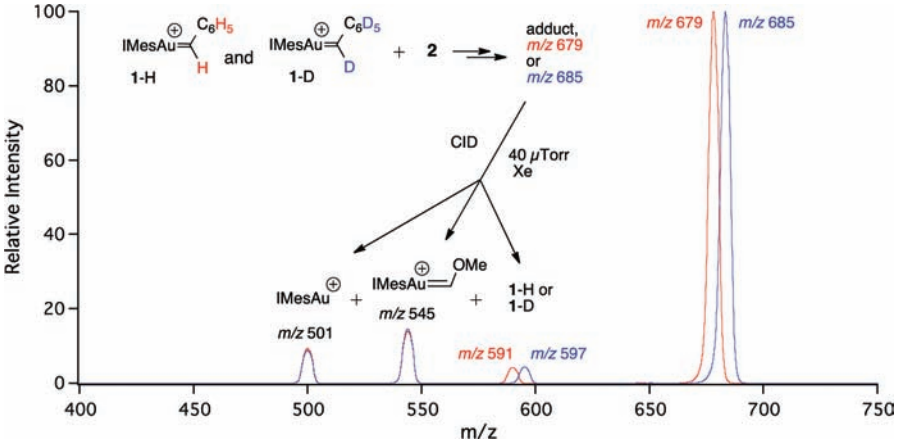

Figure 3. Overlay daughter-ion mass spectra obtained by separate CID of the adducts of **2** with benzylidenes **1**-H (red) and **1**-D (blue) at 40 μTorr xenon pressure and −60.0 V collision offset (Lab frame). Only ionic CID products are shown.

intensities for CID of *cis*-dimethoxyethylene adducts with unsubstituted benzylidene complexes **1**-H and **1**-D under various experimental conditions. Species **1**-H and **1**-D were prepared in analogy with the aforementioned method (Figure 1). As presented in Figure 3 and Table 1, the corresponding integrated intensities indicate very modest rate differences between the fragmentation reactions of adducts of **2** with benzylidene complex **1**-H versus its deuterated analogue **1**-D.

To check the robustness of the results, we compared the intensities at various collision gas pressures and collision offsets (Table 1). Interestingly, the experimental data suggests that when more excess energy is available to the gold benzylidene-olefin adduct, the minor isotope effect for cyclopropanation disappears while that for the metathesis becomes more pronounced.

DFT Calculations. Keeping in mind the experimental reference data, we now turn to the presentation and interpretation of the computational results, which were obtained for the complete IMes system. In general, because of the transient nature of gold species implicated in catalysis, theoretical studies have proven very useful in clarifying mechanistic aspects of the involved transformations.[22,23]

Table 1. Kinetic Isotope Effects with Error Bars, As Determined from the Intensity Ratios for the Competing Cyclopropanation, Metathesis, and Olefin Loss Channels

	secondary isotope effect k^H/k^D		
Xe pressure, μTorr/ collision offset, V	cyclopropanation	metathesis	olefin loss
40/−40	1.07 ± 0.06	0.96 ± 0.04	0.90 ± 0.05
40/−60	1.06 ± 0.05	0.96 ± 0.04	0.94 ± 0.04
60/−40	1.02 ± 0.03	0.92 ± 0.02	0.94 ± 0.03
60/−60	0.99 ± 0.03	0.94 ± 0.03	0.88 ± 0.03
80/−40	0.99 ± 0.03	0.91 ± 0.02	0.95 ± 0.03

The attractive interaction between starting electrophilic benzylidene[24] **1** and olefin **2** can give rise to three initial adducts **3A**−**C** (Figure 4), of which only the η^2-bound adduct **3A** is a productive intermediate leading to a global minimum on the potential energy surface (PES) in question. It is worth noting that η^1 adduct **3B** with a C_1−O contact of 2.523 Å is destabilized by

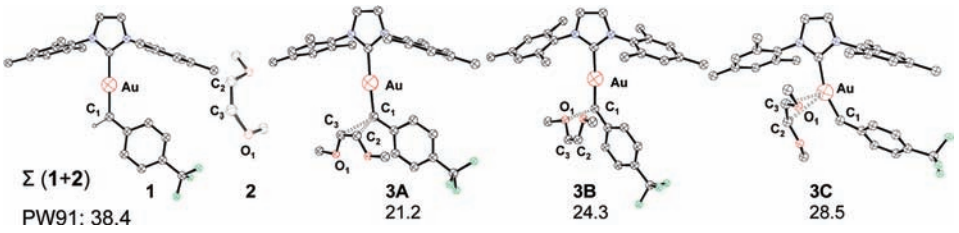

Figure 4. Reactants **1** and **2**, and possible structures of the initial adduct. Zero-point energy (ZPE) corrected energies (kcal mol^{-1}) are given relative to the global minimum **6** (*vide infra*). Selected bond lengths [Å]: **1**, Au−C_1 1.979; **2**, C_2−C_3 1.353; C_3−O_1 1.363; **3A**, Au−C_1 2.021; C_1−C_2 2.576; C_1−C_3 2.441; C_2−C_3 1.342; C_3−O_1 1.385; **3B**, Au−C_1 1.993; C_2−C_3 1.358; C_1−O_1 2.523; **3C**, Au−C_1 1.986; Au−C_2 3.041; Au−C_3 3.364; C_3−O_1 1.350.

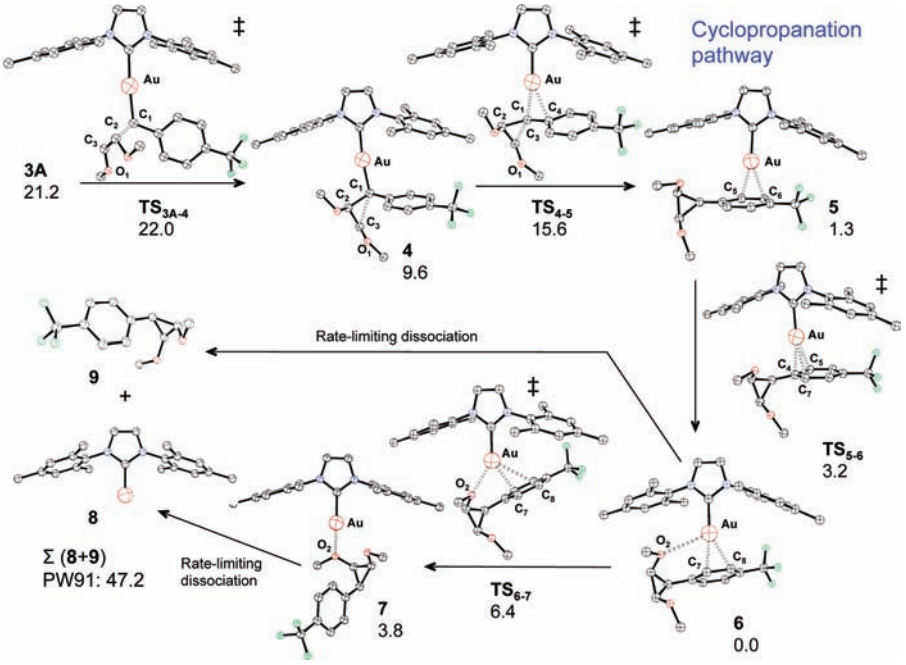

Figure 5. Located intermediates and transition states along the cyclopropanation pathway. Selected bond lengths [Å] and angles (deg): $\mathbf{TS_{3A-4}}$, Au−C_1 2.125; C_1−C_2 1.664; C_2−C_3 1.450; C_3−O_1 1.302; **4**, Au−C_1 2.155; C_1−C_2 1.597; C_2−C_3 1.462; C_1−C_3 2.209; C_3−O_1 1.298; ∠C_1−C_2−C_3 92.4; $\mathbf{TS_{4-5}}$, Au−C_1 2.462; Au−C_4 2.442; C_1−C_2 1.593; C_1−C_3 1.628; C_3−O_1 1.364; **5**, Au−C_5 2.289; Au−C_6 2.369; $\mathbf{TS_{5-6}}$, Au−C_4 2.284; Au−C_5 2.586; Au−C_7 2.614; **6**, Au−C_7 2.272; Au−C_8 2.404; Au−O_2 3.234; $\mathbf{TS_{6-7}}$, Au−O_2 2.387; Au−C_7 2.660; Au−C_8 3.241; **7**, Au−O_2 2.155.

3.1 kcal mol^{-1} with respect to η^2-bound adduct **3A**. Adduct **3C** is yet 7.3 kcal mol^{-1} higher in energy than **3A** and features a ∼0.6 Å elongation of the average C_1-**2** distance in **3A** as compared to the Au−**2** contacts in **3C**.

Figure 5 shows the intermediates and transition states that are involved in the relaxation of initial adduct **3A** to cyclopropane adduct **6**, which we identified as the global energy minimum and hence postulate as the key parent species at m/z 747 in the gas-phase experiments. The choice for a *cis* arrangement of the substituents in **6** is based on reports of *cis*-selective gold-mediated cyclopropanation,[24d,25−28] but the stereoselectivity of the cyclopropanation should not affect the basic topology of the PES. Adduct **3A** is connected to an open-chain, resonance-stabilized intermediate **4** via a very low-lying transition state $\mathbf{TS_{3A-4}}$, involving an activation energy of merely 0.8 kcal mol^{-1}. In accord with our previous report,[8] the acute central C_1−C_2−C_3 angle of 92.4° in **4** is indicative of a stabilizing interaction between the back lobe of the Au−C σ bond and the vacant p orbital of the partially carbocationic C_3 atom.[29] As a measure of the extent of charge delocalization, it is instructive to compare the C_3−O_1 distances in the intermediates and transition states on the PES under consideration. Thus, the C_3−O_1 bond distance is gradually shortening from 1.385 Å in **3A** to 1.364 Å in $\mathbf{TS_{3A-4}}$ and 1.298 Å in **4**, in accord with the formation of an oxenium-type intermediate. Due to the aforementioned orbital stabilization, the cyclopropane ring closure requires only minor geometrical changes and occurs via transition state $\mathbf{TS_{4-5}}$ with a barrier of only 6 kcal mol^{-1}. The formation of the three-membered ring is accompanied by transfer of the π-acidic gold fragment to the aryl moiety, forming a low-energy η^2-coordinated adduct **5**.[30] In turn, $\mathbf{TS_{5-6}}$ leads to the global energy minimum **6** via a very shallow barrier for a "walking" of IMesAu to the other side of the aryl ring. The extra oxygen−gold interaction present in **6** accounts for 1.3 kcal mol^{-1} stabilization and provides the thermodynamic driving force for this side switching. We have additionally checked if an alternative pathway exists where rotation of the cyclopropyl ring around the C_1−C_4 bond could connect **5** and **6**. A linear transit calculation shows that it requires higher activation

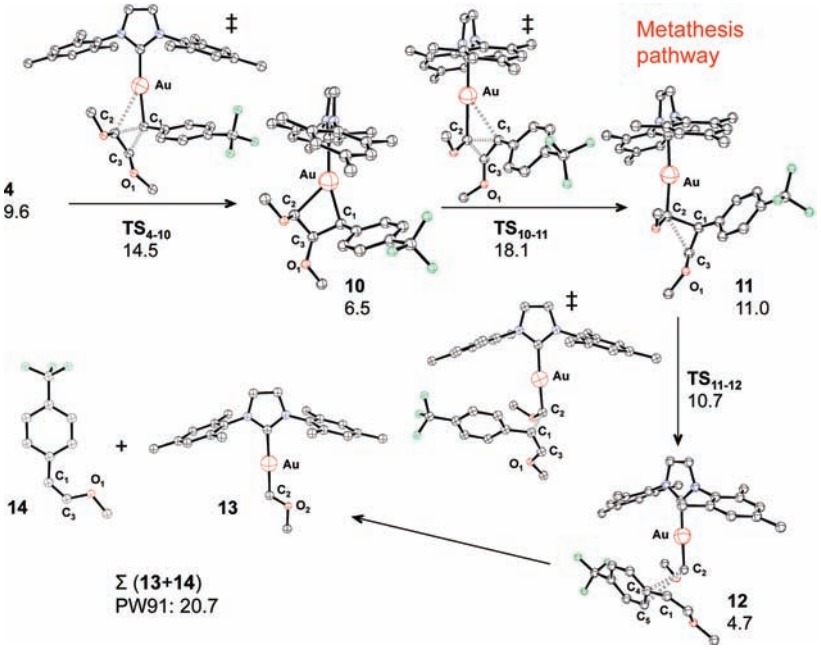

Figure 6. Located intermediates and transition states along the metathesis pathway. ZPE-corrected energies (kcal mol^{-1}) are given relative to the global minimum **6**. Selected bond lengths [Å] and angles (deg): $\mathbf{TS_{4-10}}$, Au−C_1 2.248; Au−C_2 2.936; C_1−C_2 1.659; C_2−C_3 1.450; C_1−C_3 1.723; C_3−O_1 1.349; **10**, Au−C_1 2.161; Au−C_2 2.318; C_2−C_3 1.510; C_1−C_3 1.538; C_1−C_2 2.286; C_3−O_1 1.335; ∠C_1−Au−C_2 61.3; $\mathbf{TS_{10-11}}$, Au−C_2 2.322; Au−C_1 2.835; C_1−C_2 1.652; C_2−C_3 1.483; C_1−C_3 1.577; C_3−O_1 1.373; **11**, Au−C_2 2.104; C_1−C_2 1.759; C_1−C_3 1.428; C_3−O_1 1.307; C_2−C_3 2.298; ∠C_2−C_1−C_3 91.7; $\mathbf{TS_{11-12}}$, Au−C_2 2.087; C_1−C_2 1.875; C_1−C_3 1.413; C_3−O_1 1.313; **12**, Au−C_2 1.998; C_2−C_1 3.881; C_2−C_4 3.436; C_2−C_5 3.227; **13**, Au−C_2 1.984; C_2−O_2 1.293.

energy (∼4 kcal mol^{-1}) and is thus slightly disfavored than isomerization through $\mathbf{TS_{5-6}}$. As all steps in the rearrangement of initial adduct **3A** to **6** are exothermic with barriers well below the energy of **1**+**2**, one should assume that thermalization of **1** with **2** affords **6** as the key parent ion. Subsequent decoordination of neutral cyclopropane **9** to form observed species **8** (m/z 501 in Figure 1) may occur either from the global minimum **6** or via oxygen-bound intermediate **7**, which is connected with **6** through aryl-to-alkoxy ligand exchange ($\mathbf{TS_{6-7}}$). The dissociation step is rate determining in the gas phase and overall endothermic by 47.2 kcal mol^{-1}, including zero-point energy correction, which is in good agreement with the experimental threshold of 43.6 ± 1.8 kcal mol^{-1}.

Figure 6 presents a mechanistic rationale for the apparent metathesis channel that competes with the cyclopropanation reaction. Upon collisional activation, key intermediate **6** can revert to open-chain species **4**, from which a branching can occur between the olefin dissociation and metathesis pathways. Specifically, alternative ring closure of **4** furnishes metallacyclobutane **10**,[31] and subsequent productive cycloreversion via transition state $\mathbf{TS_{10-11}}$ produces resonance-stabilized open-chain cation **11**. Transition states $\mathbf{TS_{4-10}}$ and $\mathbf{TS_{10-11}}$ are reminiscent of the conventional [2 + 2] cycloaddition that is operative with olefins and ruthenium carbenes, for instance.[32] The C_3−O bond length in both transition states is slightly longer than in **10** while in **11** this bond is again nearly as short as in **4** (1.307 Å). The central C_2−C_1−C_3 angle of 91.7° in intermediate **11** is indicative of a stabilizing overlap as discussed above for species **4**. Subsequent lengthening of the C_1−C_2 bond in **11** affords the carbene aryl adduct **12** that finally loses the olefin (**14**) to provide the experimentally observed cationic Fischer carbene **13** (m/z 545 in Figure 1). Transition state $\mathbf{TS_{11-12}}$ is extremely shallow, as reflected in its 0.3 kcal mol^{-1} lower relative energy than that of intermediate **11**. We were not able to optimize this transition state with tight SCF convergence criteria and thus attribute the latter discrepancy to an integration error. Interestingly, the C_2−O bond length in methoxymethylidene complex **13** is the shortest among all related C−O contacts presented in this work (1.293 Å), thus demonstrating a strong resonance stabilization.

While the final olefin dissociation to form **13** is endothermic by 20.7 kcal mol^{-1} relative to **6**, the preceding transition state $\mathbf{TS_{10-11}}$ is only 2.6 kcal mol^{-1} lower in energy. Recalling that the computed surface depicts potential energy and not Gibbs free energy (which would not be defined for reactions under microcanonical conditions), and recalling RRKM theory,[18] the density of states and hence the rate constant increase more rapidly with excess energy for a "loose" dissociation than for a "tight" rearrangement. Accordingly, we find it appropriate to assign traversal of $\mathbf{TS_{10-11}}$ to be the rate-determining step in the metathesis pathway, especially when the data fitting includes the T-CID curve well above threshold, as is the case in the present instance. Previously our group had found a similar situation in the case of treatment of an overall reductive elimination.[11] Thus, the experimental cross section for the metathesis should be fitted with a tight transition state model, which will afford the barrier for dissociation of products **13** and **14**. Indeed, we find excellent agreement of the computed dissociation energy of 20.7 kcal mol^{-1} with the experimental threshold of 20.3 ± 0.9 kcal mol^{-1}.

The cationic Au(I) species described in this work are isoelectronic to Hg(II) salts that react with cyclopropane derivatives by corner opening of the 3-membered ring to give cationic open-chain intermediates.[33] Hence, we have investigated if analogous intermediates and transition states also exist on the current PES, and located corresponding corner- and edge-aurated cyclopropane

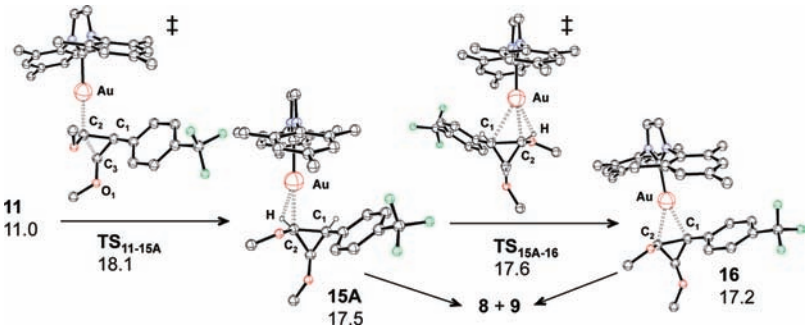

Figure 7. Ring closure to form corner- and edge-aurated cyclopropane adducts. Selected bond lengths [Å] and angles (deg): $\mathbf{TS_{11-15A}}$, Au−C_2 2.339; C_1−C_2 1.621; C_2−C_3 1.575; C_3−O_1 1.380; ∠C_2−C_1−C_3 60.6; **15A**, Au−C_2 2.336; Au−H 2.045; C_2−H 1.141; C_1−C_2 1.587; ∠C_2−Au−H 29.3; $\mathbf{TS_{15A-16}}$, Au−C_1 2.743; Au−C_2 2.339; Au−H 2.188; C_1−H 1.126; C_1−C_2 1.621; **16**, Au−C_1 2.408; Au−C_2 2.434; C_1−C_2 1.686; C_2−H 1.112.

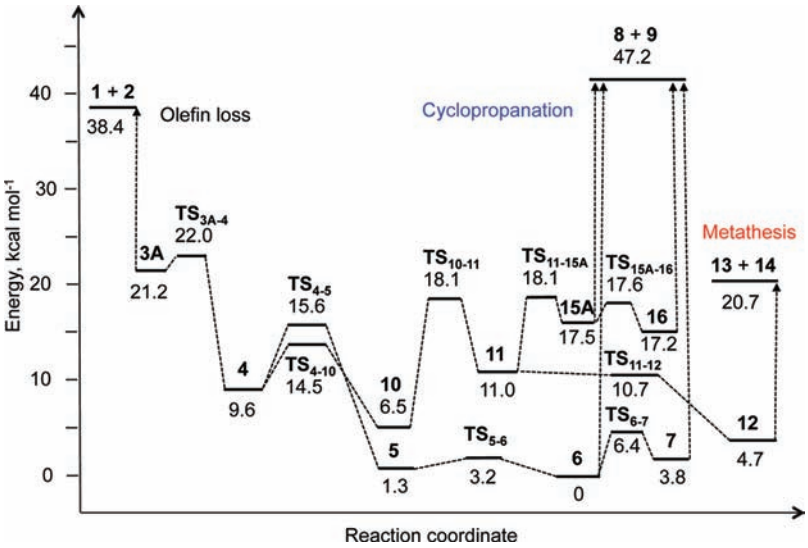

Figure 8. Schematic representation of the PES for cyclopropanation and formal metathesis of olefin **2** with gold benzylidene **1**.

adducts (Figure 7). Transition state $\mathbf{TS_{11-15A}}$ resides 6.1 kcal mol^{-1} above the open-chain intermediate **11** and connects it with an interesting corner-aurated species **15A**. Interconversion between corner- and edge-aurated cyclopropane species proceeds via a very shallow transition state $\mathbf{TS_{15A-16}}$ and requires very little geometrical change. Because of this large structural similarity, the part of the PES connecting $\mathbf{TS_{11-15A}}$ with **16** is rather flat. As compared to agostic complex **15A**, characteristic geometrical perturbations for edge-aurated intermediate **16** involve a lengthening of the central C_1−C_2 bond by 0.1 Å and expectedly a similar shortening of the C_2−H bond. Detachment of the gold fragment could occur from either adduct **15A** or **16** to produce the experimentally observed species **8**. However, since the latter process requires an overall activation energy of 47.2 kcal mol^{-1} while the metathesis is endothermic by only 20.7 kcal mol^{-1}, partitioning after **11** should predominantly favor the apparent metathesis manifold. Lastly, we point out that metathesis products **13** and **14** are also accessible in a concerted fashion from a conformer of **15A** via transition state $\mathbf{TS_{15B-13,14}}$ (shown in the Supporting Information). The associated barrier lies 22.7 kcal mol^{-1} above the global minimum **6** and is thus disfavored relative to the ring-opening via open-chain intermediate **11**, as presented in Figure 6.

DISCUSSION

Figure 8 summarizes the PES presented herein, which allows a rationalization of our previous observations on the reactivity of gold benzylidenes with electron-rich alkenes.[6−8] First, the lack of metathesis-type reactivity of gold benzylidenes with *cis*-3-hexene, as opposed to *cis*-1,2-dimethoxyethylene or other vinyl ethers, can be understood by the fact that the charge delocalization in transition states analogous to $\mathbf{TS_{4-10}}$ and $\mathbf{TS_{10-11}}$ (see also Figure 6) is less efficient for simple olefins.

Our previous linear free-energy relationship (LFER) studies on substituted gold arylidenes include two series of precursor P-ylid adducts. The findings with IMes-supported gold ylid complexes, such as that used in this work (Figure 1), demonstrated that depletion of the electron density on the arylidene fragment of **1** via variation of the *para*-substituent (R, as shown in Scheme 1 and Figure 9, left structure) results in higher rates of cyclopropanation. In contrast, the metathesis pathway was hardly affected by the electronic effects, whereas electron-donating groups facilitated the regeneration of the starting carbene **1**.[7a] When heteroleptic bis-ylid adducts $(Ph_3PCHAr)_2Au^+$ were used as precursors to complexes with the same arylidene moiety, depletion of the electron density on the supporting P-ylid ligand resulted in a lower rate for cyclopropanation while both

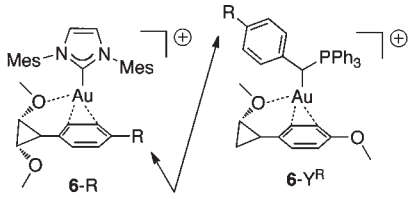

		Slopes (ρ) and uncertainties		
		Cyclopropanation	Metathesis	Olefin Loss
6-R	σ:	0.53 ± 0.12	–0.04 ± 0.11	–1.27 ± 0.14
	σ^+:	0.37 ± 0.09	–0.02 ± 0.08	–0.89 ± 0.13
6-Y^R	σ:	–0.28 ± 0.05	0.23 ± 0.04	0.23 ± 0.06

Figure 9. Comparison of two complementary LFER studies and slopes of the Hammett plots.[7]

Scheme 2. Gold-Catalyzed Transcyclopropanation Reaction Reported in Ref 25

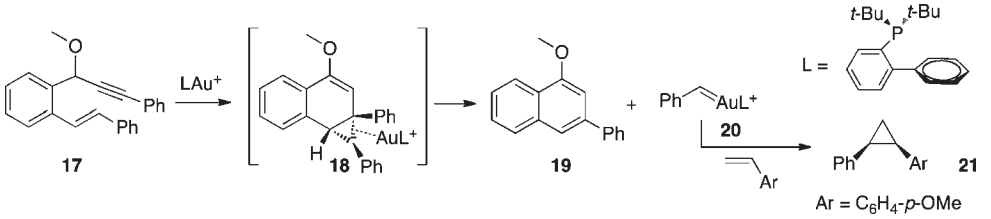

metathesis and regeneration of the starting species were accelerated with the same magnitudes of ρ (Figure 9).[7b]

The PES presented in this work confirms our previously proposed rationale[7b] for these observations. Namely, the height of the final dissociation barrier is responsible for the trends for the cyclopropanation channel, as electron-releasing substituents R on the arylidene will stabilize adduct **6**-R while raising the dissociation threshold and thus diminishing the rate to form **8** and **9**-R (Figure 5). In contrast, donating substituents R on the supporting ligand in **6**-Y^R increase the cyclopropanation rate by stabilizing the cationic gold fragment after the dissociation (Figure 9, left).

Interestingly, for the ylid-supported complexes we found the same magnitude ρ for metathesis and olefin loss to regenerate starting carbene species, which at first glance suggests an identical rate-limiting transition state for these processes.[7b] However, the most likely candidate would be the P-ylid analogue of the relatively low-lying $\mathbf{TS_{4-5}}$ (Figures 5,8) and it appears improbable that a change of the supporting ligand from IMes to P-ylid would result in a substantial elevation of this activation barrier. Instead, we explain the experimental observation from the point of view of complementary pairs of intermediates and transition states for productive and unproductive carbene exchange. Given the very close similarity between the pathways to regenerate **1** and **2** from **4** or to productively form **13** and **14** from **11**, varying the electronic properties of the supporting ligand is expected to alter the energy levels of the corresponding points on PES in a very similar fashion. Moreover, the relative energy of the transition states connecting intermediates **4** and **11** (Figure 6) would change in a similar manner as well. The comparable, small positive ρ values for the aforementioned processes are then due to the suppression of the cyclopropane dissociation from **6**-Y^R upon increasing the electron-accepting properties of the substituent R. Lastly, the suppression of olefin loss from **6**-R by electron-withdrawing substituents on the aryl group is explained by a greater energetic destabilization of the resulting electrophilic arylidenes **1**-R, which outweighs the destabilizing effect of lower π-electron density in **6**-R.

The secondary kinetic isotope effects reported herein are also consistent with the metal-bound cyclopropane species **6** being the global minimum on the PES. Namely, since breaking of the Au−aryl coordination in **6** does not affect the hybridization of the C_1-carbon atom, no obvious secondary KIE is expected, which is consistent with experiment (Table 1). Small but detectable k^H/k^D ratios of about 0.9 for the formation of gold carbene species are due to a difference in C−H bond bending ability in the cyclopropane adduct versus **1** and **13**.

Alternative Pathways for Cyclopropane Ring-Opening to Form Gold Carbene Species. The pathway presented in Figure 7 is intimately related to our results communicated earlier on the ring-opening of 1,2-dimethoxycyclopropane with Lewis acidic $IMesAu^+$ cation.[8] Also here we find that the open-chain intermediate **11** that provides the experimentally observed Fischer-type carbene **13** can be formed either via a metallacyclobutane pathway (Figure 6) or through direct auration of the three-membered ring (Figure 7). The isolobal relationship[34] between H^+ and $IMesAu^+$ offers a direct analogy of the latter process with the well-studied literature example of ring-opening of the protonated cyclopropane.[35] However, in the present case of a trisubstituted cyclopropane ring, not only are the last steps of the direct auration (**15A** → **11**) energetically disfavored, also the anticipated[8] connection between **7** and **15A** does not appear to exist at the PW91/cc-pVDZ(-PP) level of theory. We explain this by the increased steric demands in a trisubstituted cyclopropane ring versus the previously studied disubstituted system.[8] Indeed, since

Scheme 3. (Left) Stereochemical Model of Toste (TS) for the Cyclopropanation of Olefins with Gold Carbenoids Originating from Propargyl Pivaloate and (Right) Cation 22, Calculated by Echavarren As an Intermediate in the Stereoselective Cyclopropanation of Styrene

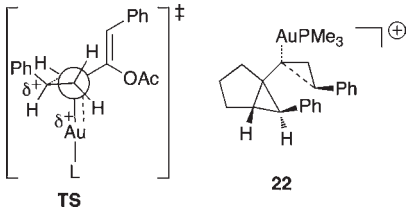

the ring-opening auration requires a stabilizing agostic interaction between the O-bound Au fragment and an adjacent C−H bond, replacement of that hydrogen atom by an aryl group renders this step energetically inaccessible. However, the possible existence of such alternative pathways is relevant for the following mechanistic discussion of selected solution-phase transformations.

Analogies with literature. As was already mentioned in the Introduction, the early work by Gassman[5] set up a precedent for "Retrocyclopropanation" reactivity with tungsten, but the observation was not followed up. Only very recently Echavarren has provided another interesting example of related solution-phase transcyclopropanation reactivity (Scheme 2).[25] Namely, in the presence of an electrophilic gold catalyst, 1,6-enynes such as **17** are converted to naphthalene derivatives (**19**) and free benzylidene gold carbene (**20**), presumably via retro-cyclopropanation of the intermediate tricyclic adduct **18**. The existence of reactive species **20** was confirmed by trapping with an external olefin to give the corresponding cyclopropane (**21**). Thus, the solution-phase transformation **18** → **19** + **20** is analogous to the reactivity observed in our gas-phase studies (*vide supra* and refs 6−8).

From the mechanistic standpoint, olefin cyclopropanation with a gold carbene species was originally proposed to follow a concerted pathway. In 2005, Toste and co-workers have suggested a transition state model (**TS**, Scheme 3, left) to account for the high level of stereocontrol found in cyclopropanated electron-rich olefins such as styrenes[26] and, closely related to the work described herein, the vinyl ether 3,4-dihydro-2H-pyran. First indications that electrophilic gold cyclopropanation might alternatively follow a stepwise process appeared shortly thereafter, when Echavarren et al. computationally found both pathways for related gold carbenes species, nonetheless favoring a concerted manifold on thermodynamic grounds.[27b] However, recent computational studies from the same group[28] established a stepwise mechanism for the cyclopropanation of styrene with gold carbenes, and the experimentally observed stereoselectivity was explained by the barrier for ring closure being lower than that for rotation around the central PhCH−CH_2 bond in intermediate **22** (Scheme 3, right). For simple aliphatic olefins such as propene and ethylene, the authors did locate transition states for a concerted carbene transfer computationally.[28] On the basis of our current results, we argue that cycloadditions of gold carbene or carbenoid complexes with polar olefins such as vinyl ethers are likely to occur in a stepwise fashion via resonance-stabilized oxenium-type cations. For electrophilic gold carbene species, selectivity arguments alone should not be taken as sufficient proof for a concerted process when substrates capable of positive charge stabilization are involved, as also suggested by Fürstner et al.[24a−c]

We also wish to point out that, while computational studies on a variety of transition metals catalyzing cyclopropanation reactions have been reported,[28,36] the surface presented above features cationic open-chain intermediates that are rather reminiscent of cycloadditions of Fischer carbenes to electron-rich dienes.[37] Our calculations demonstrate that in the case of gold(I) both corner- and edge-metalated complexes can arise (**15** and **16** in Figure 7; also see ref 8) and it appears that the ring-opening occurs only via corner-aurated species, which is in agreement with the more general corner activation for cationic or ionizable complexes.[38]

CONCLUSIONS

We described herein a combined experimental and comprehensive computational study at the PW91/cc-pVDZ(-PP) level of the gold-mediated cyclopropanation and metathesis reactivity of metal-bound cyclopropane adduct **6**. The reaction surface is in agreement with all available experimental data, demonstrating that the pathways leading to products involve several intermediates. In the gas phase, the rate-limiting process for cyclopropanation is product dissociation from the cationic metal fragment, whereas the metathesis pathway involves a few internal rearrangements with similar activation energies. Alternatively, both stepwise and concerted corner attack on the cyclopropane by the Lewis acidic gold fragment connect to the metathesis products.

As for phenomenological considerations, the use of the term "olefin metathesis" for our apparent metathesis channel does not appear appropriate. Gassman suggested to call the structurally related process brought about by a tungsten catalyst a "retro-carbene addition". We prefer "cyclopropane metathesis" which suggests a potentially useful reaction sequence. Although our results were obtained neglecting solvent effects and free energy contributions, the data suggest that cationic complexes of gold or isoelectronic d^{10} complexes could provide such a reactivity pattern.[39] On the practical side, this process implies that the action of a catalyst would lead to scrambling of the cyclopropyl substituents when two cyclopropanes are reacted. Experimental confirmation of the aforementioned inferences is yet to be observed.

ASSOCIATED CONTENT

Supporting Information. Computational details, energies, geometries, experimental distribution of ion kinetic energies, as well as energy-resolved collision-induced dissociation data and full reference 9. This material is available free of charge via the Internet at http://pubs.acs.org.

AUTHOR INFORMATION

Corresponding Author

peter.chen@org.chem.ethz.ch

Notes

[†]On leave from Department of Chemistry and Biochemistry, Texas Tech University, Lubbock, Texas 79409-1061, United States.

ACKNOWLEDGMENT

Support from the ETH Zürich and the Swiss National Science Foundation is gratefully acknowledged. A.F. thanks Dr. Erik P. A. Couzijn for helpful discussions and Mr. Giorgio Zambrino for his contributions to the T-CID measurements.

REFERENCES

(1) (a) Hérisson, J. L.; Chauvin, Y. *Makromol. Chem.* **1971**, *141*, 161–176. (b) Chauvin, Y. *Angew. Chem., Int. Ed.* **2006**, *45*, 3740–3747.

(2) (a) Calderon, N.; Chen, H. Y.; Scott, K. W. *Tetrahedron Lett.* **1967**, *34*, 3327–3329. (b) Calderon, N.; Ofstead, E. A.; Ward, J. P.; Judy, W. A.; Scott, K. W. *J. Am. Chem. Soc.* **1968**, *90*, 4133–4140. (c) Calderon, N. *Acc. Chem. Res.* **1972**, *5*, 127–132.

(3) (a) Lewandos, G. S.; Pettit, R. *J. Am. Chem. Soc.* **1971**, *93*, 7087–7088. (b) Lewandos, G. S.; Pettit, R. *Tetrahedron Lett.* **1971**, *11*, 789–793.

(4) (a) Grubbs, R. H.; Brunck, T. K. *J. Am. Chem. Soc.* **1972**, *94*, 2538–2540. (b) Biefeld, C. G.; Eick, H. A.; Grubbs, R. H. *Inorg. Chem.* **1973**, *12*, 2166–2170. (c) Grubbs, R. H.; Burk, P. L.; Carr, D. D. *J. Am. Chem. Soc.* **1975**, *97*, 3265–3267. (d) Grubbs, R. H.; Carr, D. D.; Hoppin, C.; Burk, P. L. *J. Am. Chem. Soc.* **1976**, *98*, 3478–3483.

(5) (a) Mango, F. D. *J. Am. Chem. Soc.* **1977**, *99*, 6117–6119. (b) Gassman, P. G.; Johnson, T. H. *J. Am. Chem. Soc.* **1976**, *98*, 6057–6058. (c) Gassman, P. G.; Johnson, T. H. *J. Am. Chem. Soc.* **1976**, *98*, 6058–6059.

(6) Fedorov, A.; Moret, M.-E.; Chen, P. *J. Am. Chem. Soc.* **2008**, *130*, 8880–8881.

(7) (a) Fedorov, A.; Chen, P. *Organometallics* **2009**, *28*, 1278–1281. (b) Fedorov, A.; Chen, P. *Organometallics* **2010**, *29*, 2994–3000.

(8) Batiste, L.; Fedorov, A.; Chen, P. *Chem. Commun.* **2010**, *46*, 3899–3901.

(9) Frisch, M. J.; et al. *Gaussian 09*, Revision A.02; Gaussian, Inc.: Wallingford, CT, 2009.

(10) (a) Perdew, J. P.; Chevary, J. A.; Vosko, S. H.; Jackson, K. A.; Pederson, M. R.; Singh, D. J.; Fiolhais, C. *Phys. Rev. B: Condens. Matter Mater. Phys.* **1992**, *46*, 6671–6687. (b) Figgen, D.; Rauhut, G.; Dolg, M.; Stoll, H. *Chem. Phys.* **2005**, *311*, 227–244.

(11) Couzijn, E. P. A.; Zocher, E.; Bach, A.; Chen, P. *Chem.—Eur. J.* **2010**, *16*, 5408–5415.

(12) Ervin, K. M.; Armentrout, P. B. *J. Chem. Phys.* **1985**, *83*, 166–189.

(13) Narancic, S.; Bach, A.; Chen, P. *J. Phys. Chem. A* **2007**, *111*, 7006–7013.

(14) Metal-bound ylids have been intensively employed as precursors to carbene complexes, see: (a) Brookhart, M.; Studabaker, W. B. *Chem. Rev.* **1987**, *87*, 411–432. (b) Cohen, T. *Pure Appl. Chem.* **1996**, *68*, 913–918. (c) Müller, P. *Acc. Chem. Res.* **2004**, *37*, 243–251. (d) Mangion, I. K.; Weisel, M. *Tetrahedron Lett.* **2010**, *51*, 5490–5492. (e) Gandelman, M.; Naing, K. M.; Rybtchinski, B.; Poverenov, E.; Ben-David, Y.; Ashkenazi, N.; Gauvin, R. M.; Milstein, D. *J. Am. Chem. Soc.* **2005**, *127*, 15265–15272. (f) Johnson, L. K.; Frey, M.; Ulibarri, T. A.; Virgil, S. C.; Grubbs, R. H.; Ziller, J. W. *J. Am. Chem. Soc.* **1993**, *115*, 8167–8177. (g) Weber, L.; Lücke, E. *Organometallics* **1986**, *5*, 2114–2116. (h) Sharp, P. R.; Schrock, R. R. *J. Organomet. Chem.* **1979**, *171*, 43–51. (i) van Asselt, A.; Burger, B. J.; Gibson, V. C.; Bercaw, J. E. *J. Am. Chem. Soc.* **1986**, *108*, 5347–5349. (j) Schwartz, J.; Gell, K. I. *J. Organomet. Chem.* **1980**, *184*, C1–C2.

(15) For literature examples on dual cyclopropanation−metathesis reactivity, see: (a) Basato, M.; Tubaro, C.; Biffis, A.; Bonato, M.; Buscemi, G.; Lighezzolo, F.; Lunardi, P.; Vianini, C.; Benetollo, F.; Del Zotto, A. *Chem.—Eur. J.* **2009**, *15*, 1516–1526. (b) Casey, C. P.; Burkhardt, T. J. *J. Am. Chem. Soc.* **1974**, *96*, 7808–7809. (c) Casey, C. P.; Tuinstra, H. E.; Saeman, M. C. *J. Am. Chem. Soc.* **1976**, *98*, 608–609. (d) Casey, C. P.; Polichnowsky, S. W.; Shusterman, A. J.; Jones, C. R. *J. Am. Chem. Soc.* **1979**, *101*, 7282–7292. (e) Casey, C. P.; Hornung, N. L.; Kosar, W. P. *J. Am. Chem. Soc.* **1987**, *109*, 4908–4916. (f) Monnier, F.; Vovard-Le Bray, C.; Castillo, D.; Aubert, V.; Dérien, S.; Dixneuf, P. H.; Toupet, L.; Ienco, A.; Mealli, C. *J. Am. Chem. Soc.* **2007**, *129*, 6037–6049. (g) Pakuro, N. I.; Gantmakher, A. R.; Dolgoplosk, B. A. *Izv. Acad. Nauk SSSR* **1981**, *5*, 1052–1055. (h) Mori, M.; Watanuki, S. *J. Chem. Soc., Chem. Commun.* **1992**, 1082–1084. (i) Simal, F.; Demonceau, A.; Noels, A. F.; Knowles, D. R. T.; O'Leary, S.; Maitlis, P. M.; Gusev, O. *J. Organomet. Chem.* **1998**, *558*, 163–170. (j) Noels, A. F.; Demonceau, A.; Jan, D. *Russ. Chem. Bull.* **1999**, *48*, 1206–1211. (k) Kim, B. G.; Snapper, M. L. *J. Am. Chem. Soc.* **2006**, *128*, 52–53. (l) Craenenbroeck, J. V.; Isterdael, K. V.; Vercaemst, C.; Verpoort, F. *New J. Chem.* **2005**, *29*, 942–947.

(16) (a) Armentrout, P. B. *Top. Curr. Chem.* **2003**, *225*, 233–262. (b) Armentrout, P. B.; Ervin, K. M.; Rodgers, M. T. *J. Phys. Chem. A* **2008**, *112*, 10071–10085.

(17) For T-CID measurements from our group, see refs 6, 11, 13 and: (a) Hammad, L. A.; Gerdes, G.; Chen, P. *Organometallics* **2005**, *24*, 1907–1913. (b) Moret, M.-E.; Chen, P. *Organometallics* **2007**, *26*, 1523–1530. (c) Zocher, E.; Dietiker, R.; Chen, P. *J. Am. Chem. Soc.* **2007**, *129*, 2476–2481. (d) Zocher, E.; Sigrist, R.; Chen, P. *Inorg. Chem.* **2007**, *46*, 11366–11370. (e) Torker, S.; Merki, D.; Chen, P. *J. Am. Chem. Soc.* **2008**, *130*, 4808–4814. (f) Moret, M.-E.; Serra, D.; Bach, A.; Chen, P. *Angew. Chem., Int. Ed.* **2010**, *49*, 2873–2877. (g) Fedorov, A.; Batiste, L.; Couzijn, E. P. A.; Chen, P. *ChemPhysChem* **2010**, *11*, 1002–1005. (h) Fedorov, A.; Couzijn, E. P. A.; Nagornova, N. S.; Boyarkin, O. V.; Rizzo, T. R.; Chen, P. *J. Am. Chem. Soc.* **2010**, *132*, 13789–13798. (i) Serra, D.; Moret, M.-E.; Chen, P. *J. Am. Chem. Soc.* **2011**, *133*, 8914–8926.

(18) Forst, W. *Unimolecular Reactions — A Concise Introduction*; Cambridge University Press: Cambridge, 2003.

(19) Simple ligand dissociation from an ion generally occurs via a loose transition state: see refs 17c, 17e and Armentrout, P. B.; Simons, J. *J. Am. Chem. Soc.* **1992**, *114*, 8627–8633.

(20) See the discussion in ref 11. Fitting the metathesis channel with a loose transition-state model furnishes an activation energy of 33.7 kcal mol^{-1}, which is in significant discrepancy with the computed dissociation energy (Figure 5).

(21) (a) Adlhart, C.; Hinderling, C.; Baumann, H.; Chen, P. *J. Am. Chem. Soc.* **2000**, *122*, 8204–8214. (b) Volland, M. A. O.; Adlhart, C.; Kiener, C. A.; Chen, P.; Hofmann, P. *Chem.—Eur. J.* **2001**, *7*, 4621–4632.

(22) For selected recent examples, see: (a) Wang, Z. J.; Benitez, D.; Tkatchouk, E.; Goddard, W. A.; Toste, F. D. *J. Am. Chem. Soc.* **2010**, *132*, 13064–13071. (b) Garayalde, D.; Gómez-Bengoa, E.; Huang, X.; Goecke, A.; Nevado, C. *J. Am. Chem. Soc.* **2010**, *132*, 4720–4730. (c) LaLonde, R. L.; Brenzovich, W. E.; Benitez, D.; Tkatchouk, E.; Kelly, K.; Goddard, W. A.; Toste, F. D. *Chem. Sci.* **2010**, *1*, 226–233. (d) Benitez, D.; Tkatchouk, E.; Gonzalez, A. Z; Goddard, W. A.; Toste, F. D. *Org. Lett.* **2009**, *11*, 4798–4801. (e) Alonso, I.; Trillo, B.; López, F.; Montserrat, S.; Ujaque, G.; Castedo, L.; Lledós, A.; Mascareñas, J. L. *J. Am. Chem. Soc.* **2009**, *131*, 13020–13030. (f) Correa, A.; Marion, N.; Fensterbank, L.; Malacria, M.; Nolan, S. P.; Cavallo, L. *Angew. Chem., Int. Ed.* **2008**, *47*, 718–721.

(23) For general reviews, see: (a) Hashmi, A. S. K.; Hutchings, G. J. *Angew. Chem., Int. Ed.* **2006**, *45*, 7896–7936. (b) Fürstner, A.; Davies, P. W. *Angew. Chem., Int. Ed.* **2007**, *46*, 3410–3449. (c) Gorin, D. J.; Toste, F. D. *Nature* **2007**, *446*, 395–403. (d) Muzart, J. *Tetrahedron* **2008**, *64*, 5815–5849. (e) Kirsch, S. F. *Synthesis* **2008**, *20*, 3183–3204. (f) Li, Z.; Brouwer, C.; He, C. *Chem. Rev.* **2008**, *108*, 3239–3265. (g) Jiménez-Núñez, E.; Echavarren, A. M. *Chem. Rev.* **2008**, *108*, 3326–3350. (h) Gorin, D. J.; Sherry, B. D.; Toste, F. D. *Chem. Rev.* **2008**, *108*, 3351–3378. (i) Michelet, V.; Toullec, P. Y.; Genêt, J.-P. *Angew. Chem., Int. Ed.* **2008**, *47*, 4268–4315. (j) Soriano, E.; Marco-Contelles, J. *Acc. Chem. Res.* **2009**, *42*, 1026–1036.

(24) (a) Fürstner, A.; Morency, L. *Angew. Chem., Int. Ed.* **2008**, *47*, 5030–5033. (b) Seidel, G.; Mynott, R.; Fürstner, A. *Angew. Chem., Int. Ed.* **2009**, *48*, 2510–2513. (c) Fürstner, A. *Chem. Soc. Rev.* **2009**, *38*, 3208. (d) Benitez, D.; Shapiro, N. D.; Tkachouk, E.; Wang, Y.; Goddard, W. A.; Toste, F. D. *Nat. Chem.* **2009**, *1*, 482–486.

(25) Solorio-Alvarado, C. R.; Echavarren, A. M. *J. Am. Chem. Soc.* **2010**, *132*, 11881–11883.

(26) Johansson, M. J.; Gorin, D. J.; Staben, S. T.; Toste, F. D. *J. Am. Chem. Soc.* **2005**, *127*, 18002–18003.

(27) (a) López, S.; Herrero-Gómez, E.; Pérez-Galán, P.; Nieto-Oberhuber, C.; Echavarren, A. M. *Angew. Chem. Int. Ed* **2006**, *45*, 6029–6032. (b) Nieto-Oberhuber, C.; López, S.; Muñoz, M. P.; Jiménez-Núñez, E.; Buñuel, E.; Cárdenas, D. J.; Echavarren, A. M. *Chem.—Eur. J.* **2006**, *12*, 1694–1702.

(28) Pérez-Galán, P.; Herrero-Gómez, E.; Hog, D. T.; Martin, N. J. A.; Maseras, F.; Echavarren, A. M. *Chem. Sci.* **2011**, *2*, 141–149.
(29) (a) Lambert, J. B.; Zhao, Y.; Emblidge, R. W.; Salvador, L. A.; Liu, X.; So, J.-H.; Chelius, E. C. *Acc. Chem. Res.* **1999**, *32*, 183–190. (b) Traylor, T. G.; Hanstein, W.; Berwin, H. J.; Clinton, N. A.; Brown, R. S. *J. Am. Chem. Soc.* **1971**, *93*, 5715–5725.
(30) Schmidbaur, H.; Schier, A. *Organometallics* **2010**, *29*, 2–23.
(31) Auracyclobutane is known: Dinger, M. B.; Henderson, W. *J. Organomet. Chem.* **1999**, *577*, 219–222.
(32) See, for example ref 21a and Adlhart, C.; Chen, P. *J. Am. Chem. Soc.* **2004**, *126*, 3496–3510.
(33) (a) Levina, R. Y.; Gladshtein, B. M. *Dokl. Akad. Nauk SSSR* **1950**, *71*, 65–68. (b) Shabarov, Y. S.; Sychkova, L. D.; Bandaev, S. G. *J. Organomet. Chem.* **1975**, *99*, 213–222. (c) Bandaev, S. G.; Ernazarova, Z.; Shabarov, Y. S.; Sychkova, L. D. *Zh. Org. Khim.* **1985**, *21*, 297–305. (d) Lambert, J. B.; Chelius, E. C.; Bible, R. H., Jr.; Hajdu, E. *J. Am. Chem. Soc.* **1991**, *113*, 1331–1334. (e) Kočovsky, P.; Šrogl, J.; Gogoll, A. *J. Am. Chem. Soc.* **1994**, *116*, 186–197. (f) Meyer, C.; Blanchard, N.; Defosseux, M.; Cossy, J. *Acc. Chem. Res.* **2003**, *36*, 766–772 and references therein.
(34) Schmidbaur, H.; Porter, K. In *Superacid Chemistry*; Olah, G. A., Prakash, G. K. S., Molnár, Á., Sommer, J., Eds.; Wiley: Weinheim, 2009; pp 291−308.
(35) (a) Saunders, M.; Vogel, P.; Hagen, E. L.; Rosenfeld, J. *Acc. Chem. Res.* **1973**, *6*, 53–59. (b) Battiste, M. A.; Coxon, J. M. In *The Chemistry of the Cyclopropyl Group*; Rappoport, Z. J., Ed.; Wiley and Sons: Weinheim, 1987; pp 255−305. (c) Koch, W.; Liu, B.; Schleyer, P. R. *J. Am. Chem. Soc.* **1989**, *111*, 3479–3480. (d) Chiavarino, B.; Crestoni, M. E.; Fokin, A. A.; Fornarini, S. *Chem.—Eur. J.* **2001**, *7*, 2916–2921.
(36) (a) Bernardi, F.; Bottoni, A.; Miscione, G. P. *Organometallics* **2001**, *20*, 2751–2758. (b) Rodríguez-García, C.; Oliva, A.; Ortuño, R. M.; Branchadell, V. *J. Am. Chem. Soc.* **2001**, *123*, 6157–6163. (c) Fraile, J. M.; García, J. I.; Martínez-Merino, V.; Mayoral, J. A.; Salvatella, L. *J. Am. Chem. Soc.* **2001**, *123*, 7616–7625. (d) Straub, B. F. *J. Am. Chem. Soc.* **2002**, *124*, 14195–14201. (e) Straub, B. F.; Gruber, I.; Rominger, F.; Hofmann, P. *J. Organomet. Chem.* **2003**, *684*, 124–143. (f) Suenobu, K.; Itagaki, M.; Nakamura, E. *J. Am. Chem. Soc.* **2004**, *126*, 7271–7280. (g) Soriano, E.; Ballesteros, P.; Marco-Contelles, J. *Organometallics* **2005**, *24*, 3172–3181. (h) Geng, Z.; Yan, P.; Wang, Y.; Yao, X.; Han, Y.; Liang, J. *J. Phys. Chem. A* **2007**, *111*, 9961–9968. (i) Drudis-Solé, G.; Maseras, F.; Lledós, A.; Vallribera, A.; Moreno-Mañas, M. *Eur. J. Org. Chem.* **2008**, 5614–5621. (j) Özen, C.; Tüzun, N. S. *Organometallics* **2008**, *27*, 4600–4610. (k) Wang, F.; Meng, Q.; Li, M. *Int. J. Quantum Chem.* **2008**, *108*, 945–953. (l) Özen, C.; Konuklar, F. A. S.; Tüzün, N. S. *Organometallics* **2009**, *28*, 4964–4973.
(37) (a) Wulff, W. D.; Yang, D. C.; Murray, C. K. *J. Am. Chem. Soc.* **1988**, *110*, 2653–2655. (b) Wulff, W. D.; Bauta, W. E.; Kaesler, R. W.; Lankford, P. J.; Miller, R. A.; Murray, C. K.; Yang, D. C. *J. Am. Chem. Soc.* **1990**, *112*, 3642–3659. (c) Barluenga, J.; Aznar, F.; Fernández, M. *Chem.—Eur. J.* **1997**, *3*, 1629–1637.
(38) (a) Dominelli, N.; Oehlschlager, A. C. *Can. J. Chem.* **1977**, *55*, 364–370. (b) Crabtree, R. H. *Chem. Rev.* **1985**, *85*, 245–269. (c) Blomberg, M. R. A.; Siegbahn, R. E. M.; Bäckvall, J.-E. *J. Am. Chem. Soc.* **1987**, *109*, 4450–4456. (d) Coxon, J. M.; Steel, P. J.; Whittington, B. I.; Battiste, M. A. *J. Am. Chem. Soc.* **1988**, *110*, 2988–2990.
(39) For silylene transfer from silacyclopropane to alkenes with silver catalysis, see: (a) Driver, T. G.; Woerpel, K. A. *J. Am. Chem. Soc.* **2004**, *126*, 9993–10002. (b) Naodovic, M.; Yamamoto, H. *Chem. Rev.* **2008**, *108*, 3132–3148.